

# Reconstructing the attractor of spatial and time-delayed systems from the time series of a scalar variable

Carlos Quintero-Quiroz, M. C. Torrent and Cristina Masoller

Universitat Politècnica de Catalunya, Departament de Física,  
Rambla St. Nebridi 22, 08222 Terrassa, Barcelona, Spain.

April 27, 2019

## Abstract

The space-time representation of high-dimensional dynamical systems that have a well defined characteristic time scale has proven to be very useful to deepen the understanding of such systems and to uncover hidden features in their output signals. Genuine analogies between one-dimensional (1D) spatially extended systems (1D SESs) and time delayed systems (TDSs) have been observed, including similar pattern formation and propagation of localized structures. An open question is if such analogies are limited to the space-time representation, or, if it is possible to reconstruct similar attractors, from the time series of an observed variable. In this work we address this issue by considering a bistable 1D SES and two TDSs (a bistable system and a model of two lasers with time delayed coupling). In these three examples we find that we can reconstruct the underlying attractor in a three-dimensional pseudo-space, where the evolution is governed by a polynomial potential. We also discuss the limitations of the analogy between 1D SESs and TDSs.

Real-world systems in physics, chemistry, biology, economy, etc. are typically described by a large number of equations, involving a many variables, and therefore, their dynamical evolution occurs in a high dimensional phase space. One of the most exciting discoveries in the field of dynamical systems in the last decades is that, in spite of their high dimensionality, these systems can be described by low-dimensional attractors, which can be reconstructed even if one can only observe one variable, during a finite time interval, with finite resolution and with large measurement noise. Examples of such high dimensional systems are one-dimensional spatially extended systems (1D SESs), and time delayed systems (TDSs). In a space-time representation, these systems show similar phenomena (e.g., wave propagation, pattern formation, defects and dislocations, turbulence, etc.). In this work we study the reconstruction of the attractor of these systems, from the time series of one scalar variable, and find that their attractors can be reconstructed in a three-dimensional pseudo space, where the dynamics is governed by a polynomial potential.

## 1 Introduction

The space-time representation of a dynamical system, by which a characteristic time-scale is used as a “space-like dimension”, while the evolution during many characteristic times, occurs in a “temporal dimension”, first proposed by Arecchi and co-workers in the 90s [1, 2], has proven to be extremely useful to uncover hidden space-like features, such as wave propagation, pattern formation, defects and dislocations, turbulent phenomena, etc. [3, 4, 5, 6, 7, 8, 9, 10]. For example, in the case of semiconductor lasers with feedback, which, due to the feedback delay, emit chaotic light, the space-time representation of the intensity time series has uncovered the presence of various types of spatial-like structures [11, 12, 13, 14, 15, 16, 17].

The analogy between time-delayed systems (TDSs) and one-dimensional spatially extended systems (1D SESs) is based on well-known properties, like the dimension of the attractor, which in TDSs grows linearly with the delay time,  $\tau$ , and the Lyapunov spectrum, which rescaled to  $\tau$ , is independent of  $\tau$  [19]. These features correspond to the independence of the system size found in SESs. It is then natural to ask whether such analogies also apply to their underlying attractors.

TDSs are infinite-dimensional systems because, in to obtain a solution, one needs to specify as initial condition a function in the interval  $[-\tau, 0]$  [20]. However, it has been shown that their dynamics can be described by low-dimensional attractors [21, 22, 23, 24]. To investigate the similarity of SES and TDS attractors we simulate

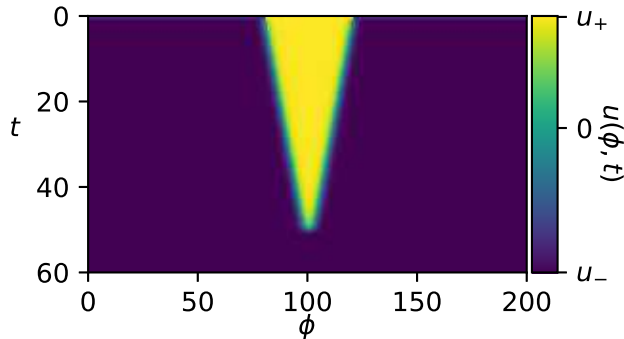


Figure 1: Space-time representation of the dynamics of the SES model, Eqs. (1) and (2) with parameters  $\alpha = 0.3$  and  $D = 4$ .

the dynamics of three model systems, one 1D SES and two TDSs, and reconstruct their attractors by using the embedding method [25].

The 1D SES is a reaction-diffusion bistable system described by a state variable  $u(\phi, t)$ ; one TDS is a scalar bistable system, described by  $u(t)$ , with a linear delayed term proportional to  $u(t - \tau)$ , and the other TDS is a model of two delay-coupled lasers, where the “observed” scalar variable is the intensity of a linear polarization one of the lasers.

Embedding methods for the reconstruction of an attractor from a time series typically use using delayed coordinates, derivatives, or principal components to define an appropriate set of independent variables from a scalar one [26, 27, 28]. Here we reconstruct the attractor of the two TDSs in a three-dimensional pseudo-space  $(x, y, z)$  by using the observed/state variable,  $x = u(t)$ , the delayed value,  $y = u_\tau = u(t - \tau)$ , and the derivative,  $z = du/dt$ . To reconstruct the attractor of the 1D SES we use the state variable  $x = u$ , and the partial derivatives,  $y = \partial_\phi^2 u$  and  $z = \partial_t u$ , computed at an arbitrary fixed time. For the three systems we show that, in the 3D pseudo-space, the systems’ evolution is well described by the equation  $z = \mathcal{F}(x, y)$ , where  $\mathcal{F}$  a simple polynomial function. Because of how  $x, y, z$  and  $\mathcal{F}$  are defined, this is expected for the scalar SES and TDS. However, for the coupled laser system, because of the complex structure of the model that includes cross-delay-coupling terms among complex variables, it is surprising that the attractor can also be described by  $z = \mathcal{F}(x, y)$ . We end with a discussion of the limitations that in practice apply to the analogy between SES and TDS attractors in the pseudo-space.

## 2 Models

### 2.1 Spatially extended system (SES)

The equation describing a reaction-diffusion 1D SES with a state variable  $u(\phi, t)$  and potential  $V(u)$  is:

$$\partial_t u = F(u) + D\partial_\phi^2 u, \quad (1)$$

where  $D$  is the diffusion coefficient and

$$\begin{aligned} F(u) &= dV(u)/du = -u(u + 1 + \alpha)(u - 1) \\ &= -u^3 - \alpha u^2 + u(1 + \alpha). \end{aligned} \quad (2)$$

Here  $V(u)$  is a double-well potential and  $\alpha$  is the asymmetry of the potential. The model has steady states at  $u = [0, u_+, u_-]$  with  $u_+ = 1$  and  $u_- = -\alpha - 1$ .

The model was simulated with spatial,  $\Delta\phi$ , and temporal,  $\Delta t$ , steps of 0.01 and 0.0001 respectively, and periodic boundary conditions. A typical evolution of the system in time is presented in Fig. 1, where the color code represents the state variable  $u(\phi, t)$  (the brightest color indicates  $u_+$  and the darkest,  $u_-$ ). Starting from an initial condition that is a rectangular pulse, we see that the system evolves in time towards the lower state of the potential,  $u_-$ .

### 2.2 Time delayed system (TDS)

We consider a TDS that has the same potential as the one-dimensional SES, and a linear feedback term with delay  $\tau$ . Such system with a state variable  $u(t)$  is described by:

$$du/dt = F(u) + \gamma u_\tau \quad (3)$$

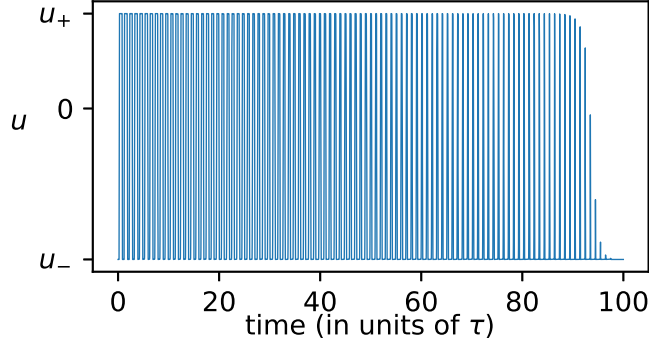


Figure 2: Time series of the TDS, Eq. (3), simulated with parameters  $\alpha = 2.5$ ,  $\gamma = 25$ ,  $\tau = 5$  and an integration step of  $\Delta t = 0.0001$ .

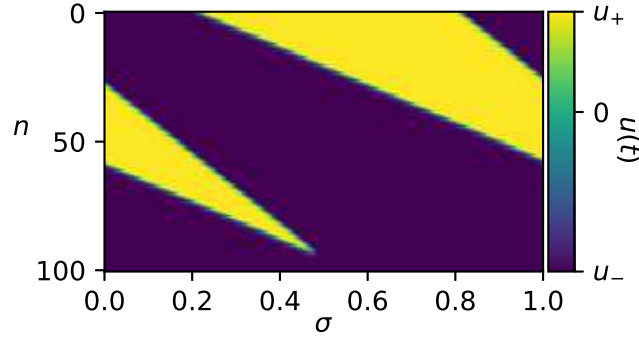


Figure 3: Space-time representation of the time series is shown in Fig. 2:  $u(t)$  with  $t = n\tau + \sigma$  is plotted in color code vs.  $n$  (the pseudo time) and  $\sigma$  (the pseudo space).

where  $F$  is given by Eq. (2),  $u_\tau = u(t - \tau)$ , and  $\gamma$  and  $\tau$  are the strength and the delay of the feedback. This system has steady states at  $(u_0, u_\pm) = \left[0, \quad (-\alpha \pm \sqrt{(\alpha + 2)^2 + 4\gamma})/2\right]$ . In order to integrate Eq. (3) it is necessary to specify an initial function on the interval  $[-\tau, 0]$ . A typical solution obtained by using an initial rectangular function with values  $u_+$  and  $u_-$  is displayed in Fig. 2. We can see that as time evolves, the time intervals during which the system remains in the higher state of the potential become gradually smaller until the system reaches the lower state of the potential. This behavior, characteristic of systems described by delay differential equations and referred to as metastability [6, 20], is the equivalent to the propagation and annihilation of fronts in SES (leading eventually to a single phase). The corresponding space-time representation is displayed in Fig. 3. Here time is expressed as

$$t = n\tau + \sigma \quad (4)$$

where  $n$  is an integer number that plays the role of time, and  $\sigma$  in  $[0, \tau)$  plays the role of the space variable  $\phi$  in the SES.

### 2.3 Coupled semiconductor lasers (CSL)

As a more complicated time-delayed system, we consider two identical lasers, with symmetric, polarization-rotated optical coupling [29, 30]. The model equations are

$$\frac{dE_{x,i}}{dt} = k(1 + j\alpha)(g_{x,i} - 1)E_{x,i} + \sqrt{\beta_{sp}}\xi_{x,i}, \quad (5)$$

$$\begin{aligned} \frac{dE_{y,i}}{dt} = & j\delta E_{y,i} + k(i + j\alpha)(g_{y,i} - 1 - \beta)E_{y,i} \\ & + \eta E_{x,3-i}(t - \tau)e^{-j\omega_0\tau} + \sqrt{\beta_{sp}}\xi_{y,i}, \end{aligned} \quad (6)$$

$$\frac{dN_i}{dt} = \gamma_N(\mu - N_i - g_{x,i}I_{x,i} - g_{y,i}I_{y,i}) \quad (7)$$

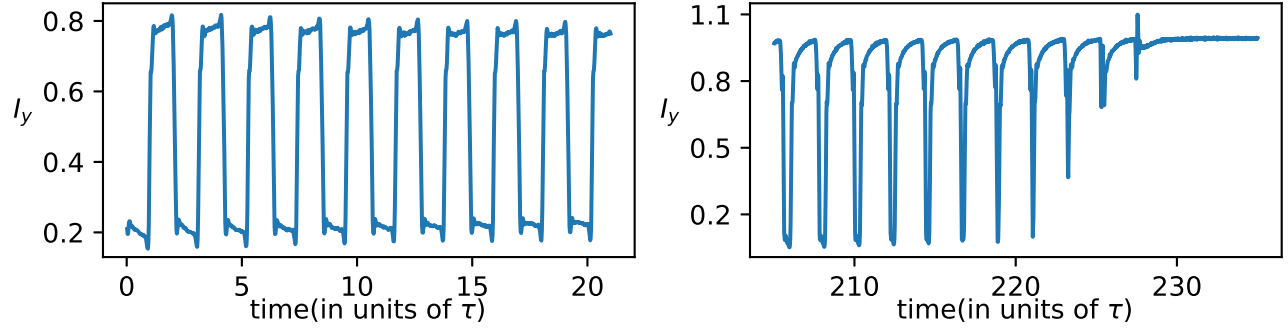


Figure 4: Time series generated by simulation of the DCSL system. The intensity of the  $y$ -polarization of laser 1,  $I = |E_{y,1}|^2$ , is plotted vs. time. The coupling strength is  $\eta = 36 \text{ ns}^{-1}$  for the top panel and  $\eta = 37 \text{ ns}^{-1}$  for the bottom panel

where  $i = [1, 2]$  denote the two lasers,  $E_{x,i}$  and  $E_{y,i}$  are the orthogonal linearly polarized complex field amplitudes (the intensities being  $I_{x,i} = |E_{x,i}|^2$  and  $I_{y,i} = |E_{y,i}|^2$  respectively), and  $N_i$  is the carrier density, of the  $i$ -th laser.  $\omega_0$  is the emission frequency of the lasers; when the lasers are uncoupled the two frequencies are the same, and are equal to the frequency of the  $x$  polarization that it is taken as the reference frequency.  $\delta$  is the frequency detuning between the  $x$  and  $y$  polarizations.  $g_{x,i}$  and  $g_{y,i}$  are the gain coefficients that include self- and cross-saturation. Other parameters are:  $k$  is the field decay rate,  $\gamma_N$  is the carrier decay rate,  $\alpha$  is the linewidth enhancement factor,  $\beta$  is the linear loss anisotropy,  $\beta_{sp}$  is the noise strength,  $\xi_{x,i}$  and  $\xi_{y,i}$  are uncorrelated Gaussian white noises and  $\mu$  is the pump current parameter.

The coupling strength and the delay time are  $\eta$  and  $\tau = L/c$ , with  $L$  being the distance between the lasers and  $c$  the speed of light. We note that polarization-rotated coupling means that cross-time-delayed terms are included in the rate equations of four complex variables:  $E_{x,1}$ ,  $E_{x,2}$ ,  $E_{y,1}$  and  $E_{y,2}$ .

Figure 4 displays an example of the intensity of the  $y$  polarization of one of the lasers, where square-wave oscillations with period  $2\tau$  are observed. Square-wave switching, which is due to the polarization-rotated coupling, can either be stable or metastable depending on the parameters. Regular and irregular switching have been observed experimentally, and the model simulations have been found to be in good agreement with the observations [29, 30].

### 3 Pseudo-space reconstruction

It is possible to re-write the Eq. (1) as

$$z = \mathcal{F}(x, y) = F(x) + Dy \quad (8)$$

where

$$x = u, \quad y = \partial_\phi^2 u, \quad z = \partial_t u. \quad (9)$$

As  $u$  is a function of the spatial variable  $\phi$  and time, the pseudo coordinates  $(x, y, z)$  are also function of space and time.

We can re-write Eq. (3) in the same form,

$$z = \mathcal{F}(x, y) = F(x) + \gamma y \quad (10)$$

where now

$$x = u, \quad y = u_\tau, \quad z = du/dt. \quad (11)$$

Using (2)  $\mathcal{F}$  can be written as

$$\begin{aligned} \mathcal{F}(x, y) &= A_0 + A_1 x + A_2 x^2 + A_3 x^3 + A_4 y \\ &+ A_5 xy + A_6 x^2 y. \end{aligned} \quad (12)$$

where

$$\begin{aligned} A_0 &= 0, \\ A_1 &= 1 + \alpha, \end{aligned}$$

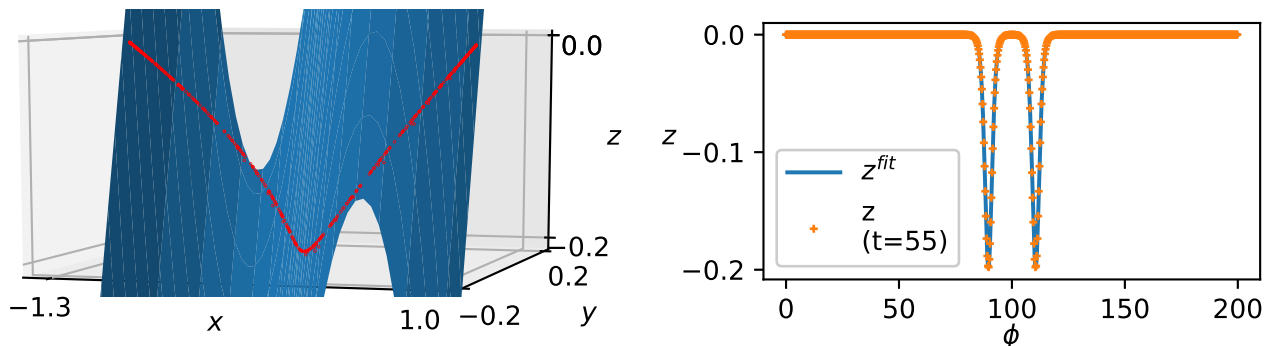


Figure 5: (a) Representation of the SES dynamics (shown in Fig. 1) in the pseudo phase space ( $x = u$ ,  $y = \partial_\phi^2 u$ ,  $z = \partial_t u$ ). The color code indicates the value of  $\mathcal{F}(x, y)$ . (b) Comparison between the numerical and the fitted time series.

$$\begin{aligned}
 A_2 &= -\alpha, \\
 A_3 &= -1, \\
 A_4 &= D \text{ for the SES,} \\
 A_4 &= \gamma \text{ for the TDS,} \\
 A_5 &= A_6 = 0.
 \end{aligned} \tag{13}$$

Therefore, the dynamics of both, the SES and the TDS are described in a three-dimensional pseudo-space, by the equation  $z = \mathcal{F}(x, y)$ , where  $\mathcal{F}$  is given in Eq. (12). We hypothesize that the coupled laser system can also be described in a similar way. Thus, to reconstruct the pseudo-spaces:

1. First, we simulate the SES and represented the dynamics in a three dimensional space, using  $[x, y, z] = [u, \partial_\phi^2 u, \partial_t u]$  as variables. Then, we fitted the trajectory to  $z = \mathcal{F}(x, y)$  and compared the fitted parameters with the theoretical ones, Eq. (13).
2. We repeat the procedure for the TDSs, using as variables  $[x, y, z] = [u, u_\tau, du/dt]$ . For the coupled laser system, the scalar variable used is the  $y$ -intensity of one laser,  $u = I_y$ .

Numerically, time and space derivatives were estimated by the 2nd order finite difference. The parameters of the function  $\mathcal{F}(x, y)$  were estimated by fitting  $z = \mathcal{F}(x, y)$ , with  $x$ ,  $y$  and  $z$  computed as Eq. (9) for the SES or as Eq. (11) for the TDSs. The `scipy.optimize.curve_fit`[31] algorithm was used to perform a non-linear least squares fit of the function  $\mathcal{F}$ , Eq. (12), to the data points.

## 4 Results

Figure 5 displays the evolution of the SES (that was shown in Fig. 1), now represented in the pseudo space  $(x, y, z)$ . The fit of the trajectory to  $z = \mathcal{F}(x, y)$  gives the parameters listed in Table 1. These values are, as expected, in excellent agreement with the theoretical values given by Eq. (13), which, for  $\alpha = 0.3$  and  $D = 3$  are also listed in Table 1. The small error (less than 3%) is attributed to the numerical estimation of the spatial and temporal derivatives.

Figure 6 displays the evolution of the TDS (that was shown in Fig. 2), now represented in the pseudo space  $(x, y, z)$ . The fit of the trajectory to  $z = \mathcal{F}(x, y)$  gives the parameters listed in Table 1. As could be expected, we again obtain an excellent agreement with the theoretical values that correspond to  $\alpha = 2.5$  and  $\gamma = 25$  (the error is less than 0.5%).

For the coupled laser system, because the model structure is more complicated, we not expected to obtain a good fit with the same polynomial function that fits the simple bistable TDS. Nevertheless, for the time series shown in Fig. 4, as shown in Fig. 7, we can fit the trajectory to  $z = \mathcal{F}(x, y)$  with the parameters given in Table 1. However, no clear relation was found between the fitted parameters and the model's parameters.

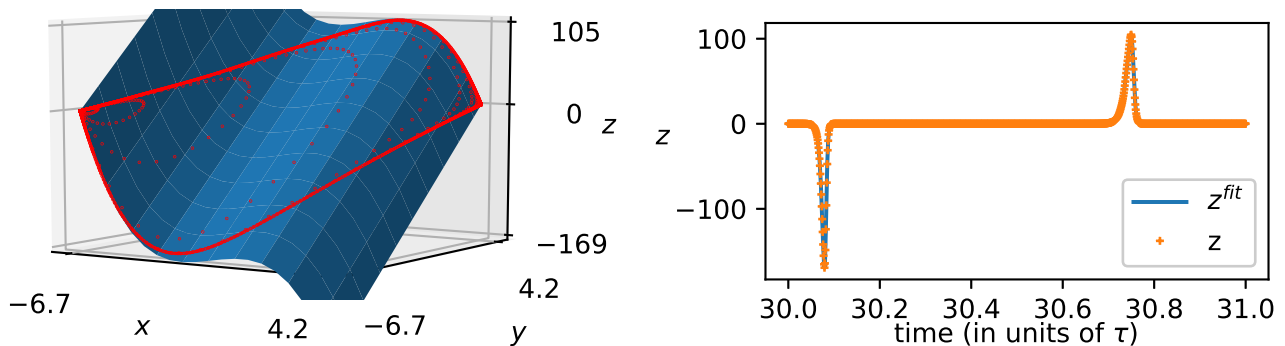


Figure 6: (a) Representation of the TDS in the phase space ( $x = u$ ,  $y = u_\tau$ ,  $z = du/dt$ ). The time-series  $u(t)$  was shown in Fig. 2. (b) Comparison between the numerical and the fitted time series.

Table 1: Theoretical and fitted parameters obtained for the SES, the TDS, the two coupled laser system (CLS) and (CLS2), and the TDS fitted as a SES (TDS2).

System	Theoretical   Fitted													
		$A_0$	$A_1$		$A_2$		$A_3$		$A_4$		$A_5$		$A_6$	
SES	0	-0.000001	1.3	1.29	-0.3	-0.29	-1	-0.99	3	2.99	0	0.0000007	0	0.0000001
TDS	0	-0.03	3.5	3.5	-2.5	-2.5	-1	-1	25	25	0	0.009	0	0.003
CLS	?	-13.7	?	92	?	-19	?	-124	?	36.1	?	-273	?	312
CLS2	?	3.9	?	8	?	37	?	-62	?	1	?	-93	?	105
TDS2	?	-1.761	?	0.082	?	0.0696	?	0.0025	?	0.00007	?	0.00001	?	-0.000005

## 5 Discussion

To test the analogy between the SES and the TDS, we tried to fit the manifold of the TDS by using the same methodology as the SES.

For this, it is necessary to compute the partial derivatives in Eq. (9), with respect to the pseudo-time and the pseudo-space variables in the space-time representation of the TDS. As it can be seen by comparing Figs. 1 and 3, there is a linear drift in the spatio-temporal representation of the TSD, which is not present in the SES. The drift is due to the fact that the oscillation period is slightly larger than  $\tau$ , and can be removed by adding a small value,  $\delta$ , to the pseudo-space variable  $\sigma$ . The spatio-temporal representation without the drift is shown in Fig. 8(a), where we note a remarkable similarity with that of the SES, shown in Fig. 1.

Nonetheless, as shown in Figs. 8(b) and (c), it is possible to obtain a reasonably good fit of the trajectory, the fitted parameters, also listed in Table 1, were not found to be in any functional relationship with those of the TDS. In Fig. 8(d) shows how the different parameters change for different values of  $\gamma$ , indicating that there is not a clear functional relationship between the estimated parameters and the theoretical ones.

We speculate that a possible reason why the SES–TDS analogy does not hold in the pseudo-space is temporal causality, which limits the similarity between the pseudo-space variable  $y_{TDS} = u_\tau = u(t - \tau)$  of the TDSs, and its counterpart of the SES,  $y_{SES} = \partial_\phi^2 u$ .  $y_{SES}$  is evaluated at fixed, arbitrary time,  $t_0$ , therefore, it is a function of the real space variable,  $x$ , and not restricted by temporal causality. Another problem is the calculation of the time derivative with respect to the pseudo-temporal variable of the TDS,  $n$  in Eq. (4), which, by definition (as  $n$  is an integer number) has a fixed time step  $\Delta t = 1$ . Therefore, it is not possible to decrease the step time in order to compute  $\Delta u$  in a small interval  $\Delta t$ .

## 6 Conclusions

We have studied the analogy between a time-delayed system (TDS) and a one-dimensional spatially extended system (SES) by considering the particular examples of a 1D reaction-diffusion SES, and a bistable scalar system with a linear delay term (TDS). We have also considered a more complicated delayed model, representing a system composed by two symmetrically coupled lasers, which involves cross-delay terms in four complex variables.

We have shown that the evolution of these systems can be described phenomenologically by the same equation in a three dimensional pseudo-phase space:  $z = \mathcal{F}(x, y)$ , where  $\mathcal{F}(x, y)$  is a polynomial function, Eq. (12), and the

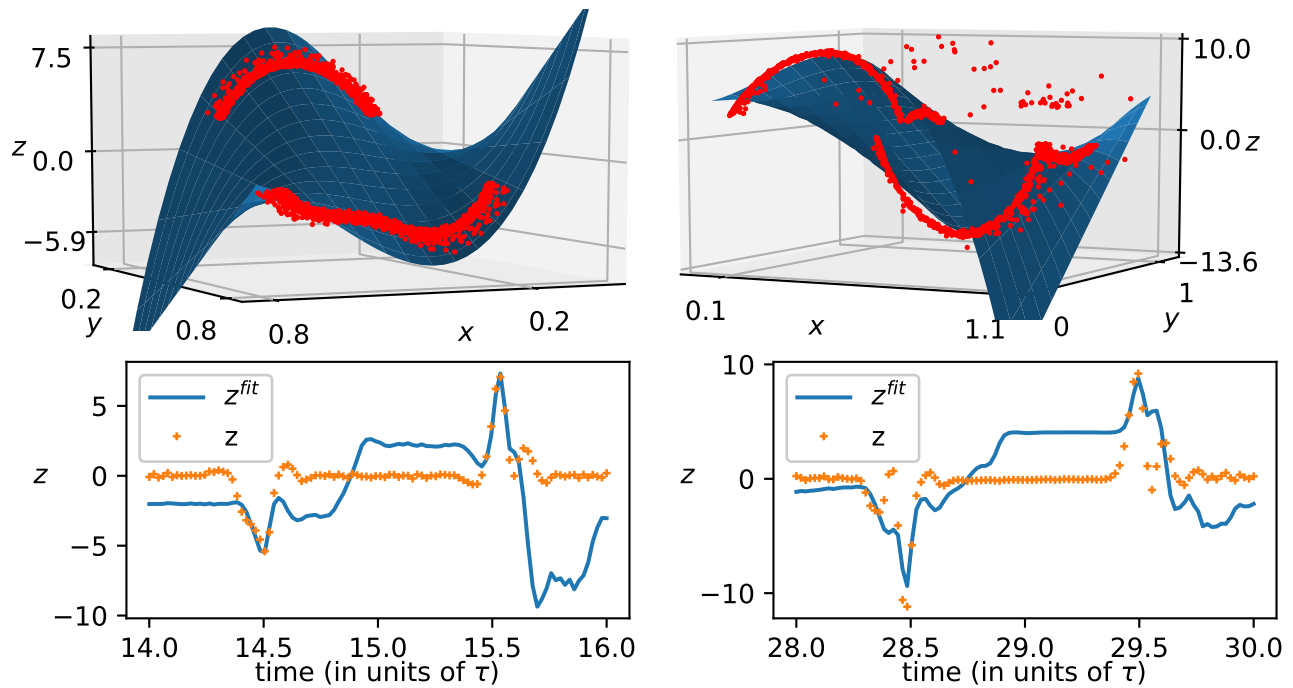


Figure 7: (a) Representation of the dynamics of the coupled laser model (the time series shown in Fig. 4), in the phase space ( $x = u$ ,  $y = u_\tau$ ,  $z = du/dt$ ) with  $u = I_y$ , together with the function  $\mathcal{F}(x, y)$ . (b) Comparison between the numerical and the fitted time series.

variables  $x$ ,  $y$  and  $z$  are defined in Eqs. (9) and (11) for the SES and for the TDSs, respectively.

In the three systems a good fit of the polynomial function  $\mathcal{F}$  was obtained. While the values of the parameters obtained for the SES and TDS were found in correspondence with the theoretical values, for the coupled lasers system the parameters were not found to be in direct correspondence with the model parameters.

While this approach could in principle be applied to any TDS or to any one-dimensional SESs, a main limitation is the estimation of the parameters of  $\mathcal{F}$ , which, in more complex SESs or TDSs, might not be limited to a low-order polynomial. Therefore, fitting  $\mathcal{F}$  can be difficult if many coefficients need to be estimated.

## Acknowledgments

This work was supported in part by ITN NETT (FP7 289146), the Spanish MINECO (FIS2015-66503-C3-2-P) and the program ICREA ACADEMIA of Generalitat de Catalunya. The authors acknowledge G. Giacomelli and F. Marino for discussions and the introduction of the problem that motivated this work. C.Q. also acknowledges G. Giacomelli and F. Marino for their hospitality during his visit to the Istituto dei Sistemi Complessi, Florence, where this work started.

## References

- [1] F. T. Arecchi, *et al.* Phys. Rev. A **45**, R4225 (1992).
- [2] G. Giacomelli and A. Politi, Phys. Rev. Lett. **76**, 2686 (1996).
- [3] S. Boccaletti, *et al.* Phys. Rev. Lett. **79**, 5246 (1997).
- [4] D. Maza, *et al.* Int. J. Bif. Chaos **8**, 1843 (1998).
- [5] T. Hikihara and Y. Ueda, Chaos **9**, 887 (1999).
- [6] M. Nizette, Physica D **183**, 220 (2003).
- [7] G. Giacomelli, *et al.* EPL **99**, 58005 (2012).

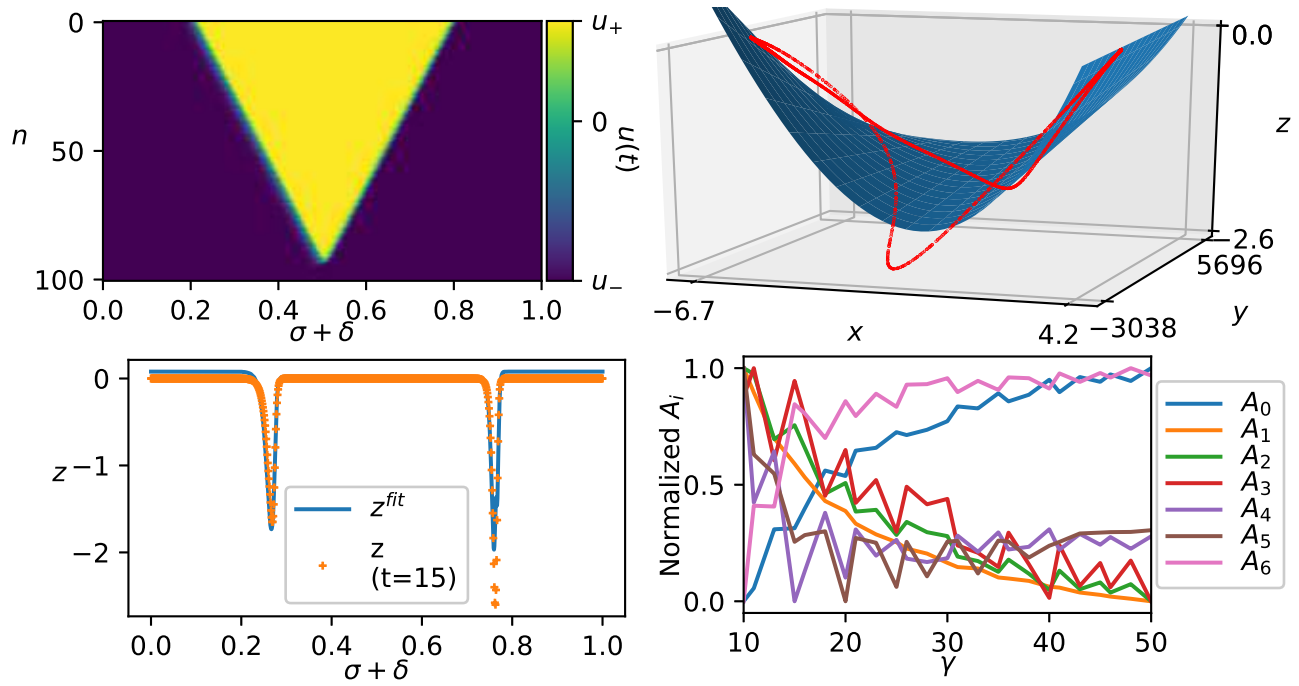


Figure 8: (a) Spatio-temporal representation of the TDS, after removing the drift. (b) Representation of the dynamics of the TDS (the time series shown in Fig. 2), in the phase space  $(x, y, z)$ , with  $x$ ,  $y$ , and  $z$  defined as in the SES, Eq. (9), with  $n$  being the “time” variable and  $\sigma$  being the “space” variable. (c) Comparison between the numerical and the fitted time series. (d) Normalized estimated parameters ( $A_i$ ) for different values of  $\gamma$ .

- [8] E. G. Turitsyna, *et al.*, Nat. Photonics **7**, 783 (2013).
- [9] L. Larger, B. Penkovsky, and Y. Maistrenko, Phys. Rev. Lett. **111**, 054103 (2013).
- [10] D. V. Churkin, *et al.* Nat. Comm. **6**, 7004 (2015).
- [11] C. Masoller, Chaos **7**, 455-462 (1997).
- [12] F. Marino, G. Giacomelli, and S. Barland, Phys. Rev. Lett. **112**, 103901 (2014).
- [13] S. Yanchuk and G. Giacomelli, Phys. Rev. Lett. **112**, 174103 (2014).
- [14] M. Marconi, *et al.* Nat. Photonics **9**, 450-U51 (2015).
- [15] J. Javaloyes, T. Ackemann, and A. Hurtado, Phys. Rev. Lett. **115**, 203901 (2015).
- [16] B. Garbin, *et al.* Chaos **27**, 114308 (2017).
- [17] F. Marino and G. Giacomelli, Chaos **27**, 114302 (2017).
- [18] H. Hicke, *et al.* Chaos **27**, 114307 (2017).
- [19] J. D. Farmer, Physica D **4**, 366 (1982).
- [20] T. Erneux, *Applied delay differential equations* (Springer 2009).
- [21] M. J. Bunner, *et al.* Phys. Rev. E **56**, 5083 (1997).
- [22] R. Hegger, *et al.* Phys. Rev. Lett. **81**, 558 (1998)
- [23] M. J. Bunner, *et al.* Eur. Phys. J. D **10**, 165 (2000).
- [24] M. J. Bunner, *et al.* Eur. Phys. J. D **10**, 177 (2000).
- [25] D. Ruelle, and F. Takens, Commun. Math. Phys. **20**, 167 (1971).

- [26] N. H. Packard, *et al.* Phys. Rev. Lett. **45**, 712 (1980).
- [27] A. M. Fraser and H. L. Swinney, Phys. Rev. A **33**, 1134 (1986).
- [28] H. Voss and J. Kurths, Phys. Lett. A **234**, 336 (1997).
- [29] C. Masoller, *et al.*, Phys. Rev. A **84**, 023838 (2011).
- [30] C. Masoller, *et al.*, Phil. Trans. R. Soc. A, **371** (2013), 20120471.
- [31] E. Jones, [www.scipy.org](http://www.scipy.org) (2016).